Waveguide transport mediated by strong coupling with atoms

Mu-Tian Cheng,[1,2,*] Jingping Xu,[1,3] and Girish S. Agarwal[1]

[1]*Institute for Quantum Science and Engineering and Department of Biological and Agricultural Engineering, Texas A&M University, College Station, Texas 77845, USA*

[2]*School of Electrical Engineering & Information, Anhui University of Technology, Maanshan 243002, People's Republic of China*

[3]*MOE Key Laboratory of Advanced Micro-Structured Materials, School of Physics Science and Engineering, Tongji University, Shanghai 200092, People's Republic of China*

(Received 2 January 2017; published 3 May 2017)

We investigate single-photon scattering properties in a one-dimensional waveguide coupled to a quantum emitter's chain with dipole-dipole interaction (DDI). The photon transport is extremely sensitive to the location of the evanescently coupled atoms. The analytical expressions of reflection and transmission amplitudes for the chain containing two emitters with DDI are deduced by using a real-space Hamiltonian. Two cases, where the two emitters symmetrically or asymmetrically couple to the waveguide, are discussed in detail. It shows that the reflection and transmission typical spectra split into two peaks due to the DDI. The Fano minimum in the spectra can be used to estimate the strength of the DDI. Furthermore, the DDI makes spectra strongly asymmetric and creates a transmission window in the region where there was zero transmission. The scattering spectra for the chain consisting of multiple emitters are also given. Our key finding is that DDI can broaden the frequency bandwidth for high reflection when the chain consists of many emitters.

DOI: 10.1103/PhysRevA.95.053807

I. INTRODUCTION

Strong coupling between photons and atoms plays important roles in quantum information processing and quantum computation. Nanocavities, which can possess ultrasmall mode volumes, are often used to realize strong coupling [1,2]. Recently, both theoretical [3,4] and experimental [5–15] works reported strong coupling between the atoms and propagating photons in a one-dimensional waveguide. Here, strong coupling means that most of the energy from the atoms decays into the propagating modes of the waveguide. Based on the strong coupling, the photon scattering properties in a one-dimensional waveguide have been extensively investigated [16–41] and are reviewed in Ref. [42]. Many quantum devices, such as single-photon switching [16–25], routers [36–38], isolation [43], transistors [35,44,45], frequency comb generators [46], and single-photon frequency converters [34] have been proposed or realized. The one-dimensional waveguide can be a photonic crystal waveguide [14], metal nanowire [5,6], superconducting microwave transmission lines [10,11], fiber [12], and diamond waveguides [15]. Atoms and cavities can play the role of scatterer. The atomic chain is also an important scatterer. The coupling between a one-dimensional waveguide and an atomic chain can lead to many interesting phenomena, such as superradiant decays [14], and changing optical band structure [47]. It can also be used to realize Bragg mirrors [48,49] and single-photon isolators [50].

It is well known that if the separation between two atoms is much smaller than the resonance wavelength, the dipole-dipole interaction (DDI) can be strong [51]. It has been shown that the DDI can change the single-photon scattering properties [52–54]. But in these studies, the two atoms are localized in one cavity [52,53] or in the same place along the waveguide [54]. The spatial separation between the two atoms along the waveguide direction is not involved. However, the separation plays an important role in some important phenomena, such as quantum beats [55], generation entanglement [56–59], single-photon switching [21], and Bragg mirrors [48,49]. Recently, Liao *et al.* investigated the time evolution of emitter excitations and photon pulses in the one-dimensional waveguide coupled to multiple emitters with DDI [60]. In this paper, we study the single-photon scattering properties by using the real-space Hamiltonian. The analytical expressions for reflection and transmission amplitudes for the case of two quantum emitters (QEs) with DDI are given. The single-photon scattering properties for many QEs with DDI are also exhibited. The results show that the DDI can significantly affect single-photon scattering properties.

The structure of this paper is organized as follows. In Sec. II, we present the model of single-photon transport in a waveguide coupled to atoms. In Sec. III, we recall the known results for the case of a single atom. In Sec. IV, we present features of the two-atom coupling. In Sec. V, we discuss the trend for many atoms, with conclusions in Sec. VI.

II. MODEL AND HAMILTONIAN

The system considered in this paper is shown in Fig. 1. N QEs with equal separation L side-couple to a waveguide. The QEs are modeled as two-level systems with ground state $|g\rangle$ and excited state $|e\rangle$. The transition frequency of the QEs is ω_A.

When ω_A is much larger than the cutoff frequency ω_c of the waveguide, the dispersion relation of the waveguide near the resonant frequency can be taken as linear [26]. Then the Hamiltonian in the real space is given by $H = H_f + H_i + H_d$, with $\hbar = 1$ [26,56],

$$H_f = iv_g \int dx \left(a_L^\dagger(x) \frac{\partial a_L(x)}{\partial x} - a_R^\dagger(x) \frac{\partial a_R(x)}{\partial x} \right) + \sum_{j=1}^{N} (\omega_A - i\Gamma'_{0j}/2)\sigma_{ee}^{(j)}, \quad (1)$$

*mtcheng@ahut.edu.cn

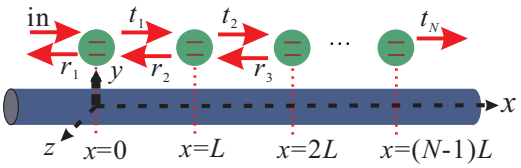

FIG. 1. The system considered in the manuscript. A chain of N QEs with equal separation L coupled to one-dimensional waveguide.

being the free propagation photon in the waveguide and the QEs; v_g is the group velocity of the photon, and $a_R^\dagger(x)$ [$a_L^\dagger(x)$] means creation of a right-propagating (left-propagating) photon at x. $\sigma_{ee}^{(j)} = |e\rangle_j\langle e|$. We have supposed that all the transition frequencies of the atoms are the same and the energy of the QE's ground state is zero. $\Gamma_{0j}^{'}$ is the energy decay rate into the nonwaveguide modes, and

$$H_i = \sum_{j=1}^{N} J_j \int dx\{\delta(x-x_j)[a_R^\dagger(x)+a_L^\dagger(x)]\sigma_j + \text{H.c.}\} \quad (2)$$

denotes the interaction between the QEs and the waveguide photon. J_j is the coupling strength between the jth QE and the waveguide photon. $\sigma_j = |g\rangle_j\langle e|$ is the ladder operator for the jth QE. Finally,

$$H_d = \Omega_{i,j} \sum_{i,j=1}^{N} (\sigma_i^\dagger \sigma_j + \sigma_j^\dagger \sigma_i) \quad (3)$$

describes the DDI. $\Omega_{ij} = \frac{3}{4}\Gamma_0[(\frac{\cos x}{x^3} + \frac{\sin x}{x^2} - \frac{\cos x}{x}) + \cos^2\theta(\frac{\cos x}{x} - \frac{3\cos x}{x^3} - \frac{3\sin x}{x^2})]$ is the DDI strength between the ith QE and the jth QE [51]. $x \equiv \frac{\omega_A}{c}|\vec{r}_i - \vec{r}_j|$. $\cos^2\theta = (\frac{\vec{p}\cdot(\vec{r}_i-\vec{r}_j)}{|p|\cdot|\vec{r}_i-\vec{r}_j|})^2$, where $\vec{r}_j$ is the location coordinate of the jth QE and $\vec{p}$ is the dipole. We suppose that all the QEs have the same dipoles and their directions are all in $-y$. Γ_0 is the decay rate of QE in free space, which is taken about 7.5 MHz in the following calculations.

Since only one excitation exists in this system, the eigenstate of H takes the form

$$|E_k\rangle = \int dx[\phi_{kR}(x)a_R^\dagger(x) + \phi_{kL}(x)a_L^\dagger(x)]|0,g\rangle + \sum_{j=1}^{N} e_k^{(j)}|0,e_j\rangle, \quad (4)$$

where $E_k = \hbar\omega_k$ is the eigenvalue of H; $|0,g\rangle$ represents all the QEs in the ground state and no photon in the system, $|0,e_j\rangle$ denotes no photon in the system and the jth QE in the excited state $|e\rangle$ while all other QEs are in the ground state, $e_k^{(j)}$ is the probability amplitude of the state $|0,e_j\rangle$, and $\phi_{kR}(x)$ and $\phi_{kL}(x)$ are the amplitudes of the fields going to the right and left in the waveguide. These are continuous except at the positions of the atoms and thus we write these in the form [26,27]

$$\phi_{kR}(x) = \begin{cases} e^{ikx}, & x < 0 \\ t_j e^{ik(x-jL)}, & (j-1)L < x < jL \\ t_N e^{ik(x-NL)}, & x > (N-1)L, \end{cases} \quad (5)$$

and

$$\phi_{kL}(x) = \begin{cases} r_1 e^{-ikx}, & x < 0 \\ r_{j+1} e^{-ik(x-jL)}, & (j-1)L < x < jL \\ 0, & x > (N-1)L, \end{cases} \quad (6)$$

where t_j and r_j are the coefficients to be determined. Substituting Eqs. (5) and (6) into the Schrödinger equation $H|E_k\rangle = E_k|E_k\rangle$, we obtain [26]

$$t_j e^{-ikL} - t_{j-1} + \frac{iJ_j e_k^{(j)}}{v_g} = 0, \quad (7a)$$

$$r_{j+1}e^{ikL} - r_j - \frac{iJ_j e_k^{(j)}}{v_g} = 0, \quad (7b)$$

$$t_{j-1} + r_j + \frac{\sum_{i=1}^{j-1}\Omega_{j,i}e_k^{(i)} + \sum_{i=j+1}^{N}\Omega_{j,i}e_k^{(i)}}{J_j} - \frac{(\Delta_k^{(j)} + i\Gamma_{0j}^{'}/2)e_k^{(j)}}{J_j} = 0, \quad (7c)$$

where $\Delta_k^{(j)} = \omega_k - \omega_A^{(j)}$. $t_0 = 1$ and $r_{N+1} = 0$ are used in the following calculations. Clearly from Eqs. (5) and (6), the transmission and reflection coefficients will be $t = t_N e^{-ikNL}$ and $r = r_1$, respectively.

III. SINGLE EMITTERS

Before showing how DDI affects the single-photon scattering properties, we review a single photon scattered by one

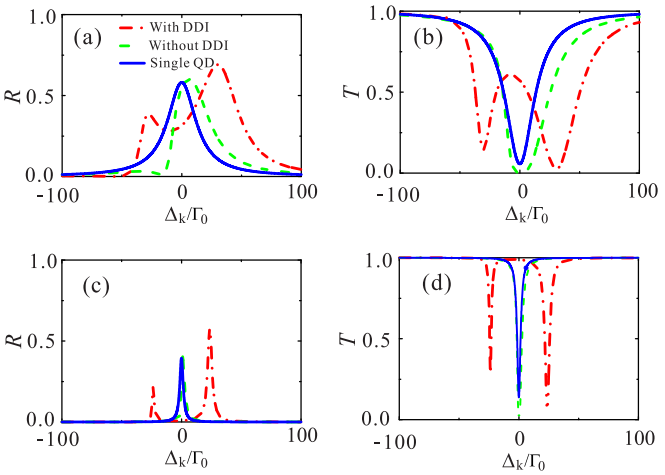

FIG. 2. R and T as a function of Δ_k. The solid blue lines are the results for single QDs. The dash-dotted red lines denote the results for a pair of QDs with DDI and the dashed green lines for a pair of QDs without DDI. In (a) and (b), the two QDs are located at $\vec{r}_1(x,y,z) = (0,\ 17\,\text{nm},\ 0)$ and $\vec{r}_2(x,y,z) = (32.75\,\text{nm},\ 17\,\text{nm},\ 0)$, respectively, corresponding to the separation between the two QDs, $L = \lambda_{qd}/20$. $\Gamma = 11.03\Gamma_0$ and $\Gamma_0^{'} = 6.86\Gamma_0$ are used in the calculations. In (c) and (d), the two QDs are placed at $\vec{r}_1(x,y,z) = (0,\ 37\,\text{nm},\ 0)$ and $\vec{r}_2(x,y,z) = (32.75\,\text{nm},\ 37\,\text{nm},\ 0)$, respectively. $\Gamma = 1.06\Gamma_0$ and $\Gamma_0^{'} = 1.26\Gamma_0$. The single QD is located at (0, 17 nm, 0) and (0, 37 nm, 0) when the solid blue lines are plotted in (a) and (b) and in (c) and (d), respectively. In the calculations, $\Omega = 23.08\Gamma_0$.

QE first. The single-photon transmission and reflection amplitudes are, respectively, given by [16,37]

$$t = \frac{\Delta_k + i\Gamma_0'/2}{i\Gamma + \Delta_k + i\Gamma_0'/2}, \tag{8a}$$

$$r = \frac{-i\Gamma}{i\Gamma + \Delta_k + i\Gamma_0'/2}, \tag{8b}$$

where $\Delta_k = \omega_k - \omega_A$ and $\Gamma = J^2/v_g$. Equations (8a) and (8b) show that reflection probability $R \equiv |r|^2$ reaches the maximum and transmission probability $T \equiv |t|^2$ reaches the minimum when $\Delta_k = 0$.

The solid blue lines in Fig. 2 exhibit the numerical results T and R with different coupling strengths between the QE and the photon in the nanowaveguide. In the numerical model, a semiconductor quantum dot (QD) with resonant wavelength $\lambda_{qd} = 655$ nm (transition frequency $\omega_A/(2\pi) \approx 457.7$ THz) is placed near a Ag nanowire, which was realized in experiments [5]. The radius of the Ag nanowire is 10 nm, and the corresponding wavelength of the propagating surface plasmon (SP), λ_{sp}, is about 211.8 nm [3], which is much shorter than the resonant wavelength of the QD due to the reduced group velocity. The spontaneous emission rate Γ_{pl} into the propagation surface plasmon modes; the energy loss rate Γ_0', which consists of radiating into the free space rate Γ_{rad}; and the nonradiative emission rate into the Ag nanowire, Γ_{nonrad}, are calculated by using the formulas given in Ref. [3].

IV. TWO QUANTUM EMITTERS

A. Symmetric coupling

We now show how the DDI affects the single-photon scattering properties for the case of a pair of QEs coupling to the waveguide. First, we discuss the results for the symmetric coupling ($J_1 = J_2 = J$). From Eqs. (7a)–(7c), one can obtain the analytical solutions to t and r, which are given by

$$t = \frac{e^{-ikL}\{-i\Gamma\Omega + ie^{2ikL}\Gamma\Omega + e^{ikL}[(\Delta_k + i\Gamma_0'/2)^2 - \Omega^2]\}}{(-1+e^{2ikL})\Gamma^2 + 2i\Gamma(\Delta_k + i\Gamma_0'/2 + e^{ikL}\Omega) + (\Delta_k + i\Gamma_0'/2)^2 - \Omega^2}, \tag{9a}$$

$$r = \frac{(1-e^{2ikL})\Gamma^2 - i\Gamma[(1+e^{2ikL})(\Delta_k + i\Gamma_0'/2) + 2e^{ikL}\Omega]}{(-1+e^{2ikL})\Gamma^2 + 2i\Gamma(\Delta_k + i\Gamma_0'/2 + e^{ikL}\Omega) + (\Delta_k + i\Gamma_0'/2)^2 - \Omega^2}, \tag{9b}$$

where Ω is the DDI strength between the two QEs. When $\Omega = 0$, which means that DDI is not considered, one can obtain

$$t = \frac{(\Delta_k + i\Gamma_0'/2)^2}{(-1+e^{2ikL})\Gamma^2 + 2i\Gamma(\Delta_k + i\Gamma_0'/2) + (\Delta_k + i\Gamma_0'/2)^2}, \tag{10a}$$

$$r = \frac{(1-e^{2ikL})\Gamma^2 - i\Gamma(1+e^{2ikL})(\Delta_k + i\Gamma_0'/2)}{(-1+e^{2ikL})\Gamma^2 + 2i\Gamma(\Delta_k + i\Gamma_0'/2) + (\Delta_k + i\Gamma_0'/2)^2}, \tag{10b}$$

which is consistent with previous reports [55,61].

Note that we can write the denominator in Eq. (10a) as $(\Delta_k + \frac{i\Gamma_0'}{2} + i\Gamma)^2 + \Gamma^2 e^{2ikL}$. The term $\Gamma^2 e^{2ikL}$ arises from the waveguide-mediated interactions between two QEs even if the direct DDI is $\Omega = 0$. Thus, it plays the role of waveguide-mediated DDI. To show this, if we drop $\Gamma^2 e^{2ikL}$, then transmission $t^{(2)}$ for the two-QE case is the square of the transmission $t^{(1)}$ for the single-QE case. Thus, in the absence of the $\Gamma^2 e^{2ikL}$ term, the field transmitted by the first QE is transmitted by the second QE, leading to the result $t^{(2)} = (t^{(1)})^2$. However, the physics is different. The field reflected by the second QE affects the first QE by changing its transmission, which then changes the fields produced by the second QE. In principle, one has a whole series of such processes and this just happens to be the physics of DDI. Hence we refer to the term $\Gamma^2 e^{2ikL}$ as waveguide-mediated DDI. We have checked that this DDI affects line shapes but does not produce splitting.

The transmission and reflection spectra for the case of $|\vec{r}_1 - \vec{r}_2| = \lambda_{qd}/20$ are shown in Fig. 2. Here, $kL \approx 0.31\pi$, which is due to the short wavelength of the SP. Without considering the DDI, the reflection spectrum reaches the maximum at $\Delta_k = 0$ and a Fano line shape appears [61]. Compared to the single-QE case, the two-QE spectra display considerable asymmetries even in the absence of DDI. The position of the Fano minimum can be estimated from the zero of the numerator in Eq. (9b). For $\Gamma_0' = 0$, it is found to occur at $\Delta_k = \Delta_k^{r\,\min} = -\Gamma(\tan kL + \frac{\Omega}{\Gamma}\sec kL)$, which depends on the strength of the DDI. Clearly, the position of the Fano minimum can be used to get an estimate of the DDI strength and this is displayed more clearly in Fig. 3. The distance between the two dips in Fig. 3 is related to $\Omega \sec kL$. The Fano line shapes in the reflection spectra are reduced strongly

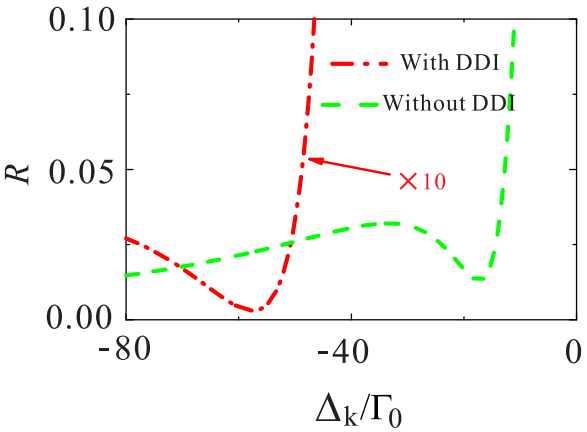

FIG. 3. Fano shape of the reflection spectrum [the region of minimum in Fig. 2(a)].

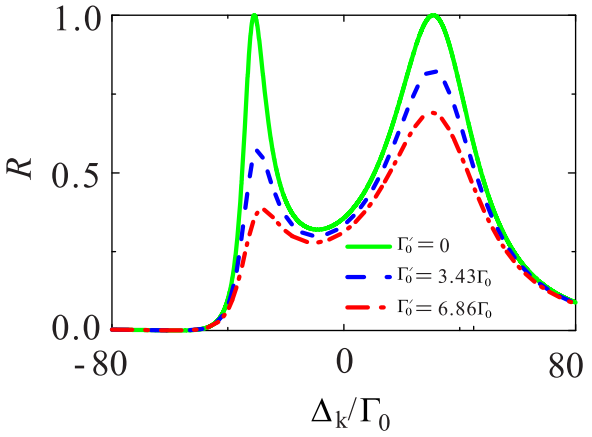

FIG. 4. Reflection spectra for the two identical QDs with different decays. In the calculations, $\Gamma = 11.03\Gamma_0$, $L = 32.75$ nm, and $\Omega = 23.08\Gamma_0$.

but still exist. Equations (9a) and (9b) also give that the single-photon reflection spectrum splits into two main peaks at $\Delta_k = \Delta_k^{r\,\max} = \pm\sqrt{2\Gamma\Omega\sin(kL)+\Omega^2}$ when $\Gamma_0^{'} = 0$. These values give the positions where $R = 1, T = 0$. Note that $\Delta_k^{r\,\max}$ depends on both DDI and kL but the DDI is absolutely essential for $\Delta_k^{r\,\max} \neq 0$. These also correspond to the positions of dips in the transmission spectrum. The differences of the main peaks of the reflection spectrum in Fig. 2 result from the energy losses. To show this claim clearly, we present Fig. 4, which shows that when energy loss is zero, both of the peaks reach the maximum of one. However, when the energy loss increases from $3.43\Gamma_0$ to $6.86\Gamma_0$, the difference between the heights of the two peaks increases from about 0.25 to about 0.31. In the numerical calculations, we take $kL = (\omega_A + \Delta_k)/v_g \approx 2\pi L/\lambda_{\rm sp}$ since $\omega_A \gg \Gamma_0$ and Δ_k [21,26].

Many reports show that single-photon scattering properties and their applications such as single-photon switching and generation entanglement are strongly related to the distance between two QEs. The DDI strength also depends strongly on the distance between the two QEs. Figure 5(a) shows Ω as a function of L for the two QDs with resonant wavelength $\lambda_{\rm qd} = 655$ nm. The Ω decreases from $23.08\Gamma_0$ to $0.28\Gamma_0$ as L increases from 32.75 to 240 nm. Figures 5(b) and 5(c) exhibit single-photon reflection spectra for $L = 52.95$ nm (corresponding to $L = \lambda_{\rm sp}/4$, $kL = \pi/2$) and $L = 105.9$ nm (corresponding to $L = \lambda_{\rm sp}/2$, $kL = \pi$), respectively. It indicates that DDI can play significant roles even though the separation between the two QDs reaches $L = \lambda_{\rm sp}/4$. However, when the distance increases to $L = \lambda_{\rm sp}/2$, the influence of DDI can be neglected; i.e., the numerical results with and without DDI are almost indistinguishable but not identical.

It is necessary to point out that spatial separation between the two QDs along the waveguide direction plays an important role in splitting the reflection spectrum. There are special cases when the DDI yields a shift in spectrum rather than splitting. This happens when the numerator and denominator

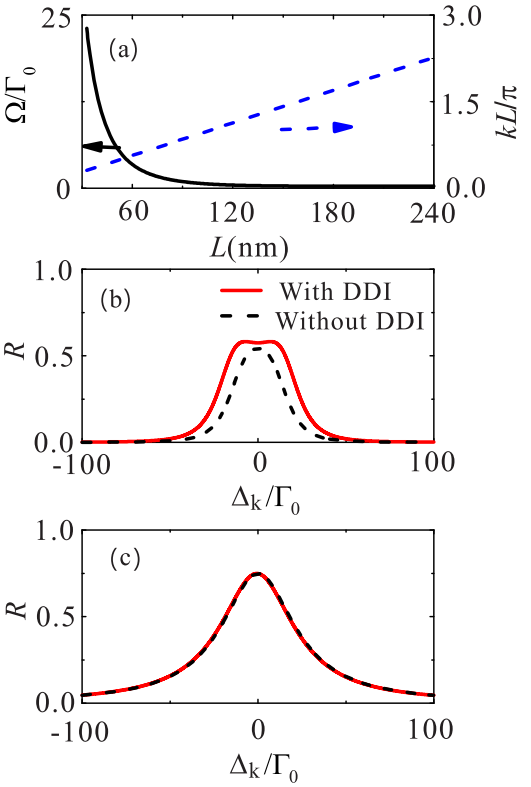

FIG. 5. (a) DDI strength as a function of the distance L between the two QDs, i.e., dots located at (x,y,z) and $(x+L,y,z)$. Single-photon reflection spectra for the case of (b) $L = \lambda_{\rm sp}/4 = 52.95$ nm and (c) $L = \lambda_{\rm sp}/2 = 105.9$ nm. In (b), $\vec{r}_1(x,y,z) = (0, 17\,\text{nm}, 0)$, $\vec{r}_2(x,y,z) = (52.95\,\text{nm}, 17\,\text{nm}, 0)$, and $\Omega = 5.12\Gamma_0$. In (c) $\vec{r}_1(x,y,z) = (0, 17\,\text{nm}, 0)$, $\vec{r}_2(x,y,z) = (105.9\,\text{nm}, 17\,\text{nm}, 0)$, and $\Omega = 0.61\Gamma_0$. In both (b) and (c), $\Gamma = 11.03\Gamma_0$ and $\Gamma_0^{'} = 6.86\Gamma_0$.

share a common zero. As an example if $kL = 0$, which can be realized, for example, for the two QDs located at $\vec{r}_1(x,y,z) = (0,0,37\,\text{nm})$ and $\vec{r}_2(x,y,z) = (0,37\,\text{nm},0)$, respectively, then $t = (\Delta_k - \Omega + i\Gamma_0^{'}/2)/[(\Delta_k - \Omega + i\Gamma_0^{'}/2) + 2i\Gamma]$, and $r = -2i\Gamma/[(\Delta_k - \Omega + i\Gamma_0^{'}/2) + 2i\Gamma]$. The collective behavior is still present as the effective linewidth parameter is changed from Γ to 2Γ. There is no splitting in the reflection spectrum but the location of the peak in the reflection spectrum shifts to $\omega_k = \omega_A + \Omega$. A similar result is obtained for $kL = \pi$; one needs to replace Ω by $-\Omega$. Thus, the relative phase factor kL produced by the propagation of the light from QE 1 and to QE 2 is important in the transport of light through a waveguide coupled to QEs.

B. Asymmetric coupling

We now discuss the single-photon scattering with asymmetric coupling. If the distances between the surface of the nanowire and the two QDs are different, then the coupling strengths $J_1 \neq J_2$. From Eqs. (7a)–(7c), one can get

$$t = \frac{e^{-ikL}\{-i\sqrt{\Gamma_1\Gamma_2}\Omega + ie^{2ikL}\sqrt{\Gamma_1\Gamma_2}\Omega + e^{ikL}(\delta_k^{(1)}\delta_k^{(2)} - \Omega^2)\}}{(-1+e^{2ikL})\Gamma_1\Gamma_2 + i(\Gamma_1\delta_k^{(2)} + \Gamma_2\delta_k^{(1)}) + 2ie^{ikL}\sqrt{\Gamma_1\Gamma_2}\Omega + \delta_k^{(1)}\delta_k^{(2)} - \Omega^2}, \tag{11a}$$

$$r=\frac{(1-e^{2ikL})\Gamma_1\Gamma_2-ie^{2ikL}\Gamma_2\delta_k^{(1)}-i\Gamma_1\delta_k^{(2)}-2ie^{ikL}\sqrt{\Gamma_1\Gamma_2}\Omega}{(-1+e^{2ikL})\Gamma_1\Gamma_2+i\left(\Gamma_1\delta_k^{(2)}+\Gamma_2\delta_k^{(1)}\right)+2ie^{ikL}\sqrt{\Gamma_1\Gamma_2}\Omega+\delta_k^{(1)}\delta_k^{(2)}-\Omega^2}, \tag{11b}$$

where $\Gamma_j=J_j^2/v_g$, $\delta_j=\Delta_k+i\Gamma_{0j}^{'}/2$ $(j=1,2)$. Equations (11a) and (11b) indicate that when $\Delta_k^2=\sqrt{\Gamma_1\Gamma_2}\Omega\sin(kL)+\Omega^2$ is satisfied, $T=0$ and $R=1$ if $\Gamma_{0j}^{'}=0$. Furthermore, if $L=0$, which can be realized for the two QDs with the same location coordinates x,z but different y, the condition changes to be $\Delta_k^2=\Omega^2$. This means that the distance between the two peaks in the reflection spectrum is dependent not only on the coupling strength via Γ but also on Ω. However, if $\Omega=0$, Eqs. (11a) and (11b) degenerate into

$$t=\frac{\delta_k^{(1)}\delta_k^{(2)}}{(-1+e^{2ikL})\Gamma_1\Gamma_2+i\left(\Gamma_1\delta_k^{(2)}+\Gamma_2\delta_k^{(1)}\right)+\delta_k^{(1)}\delta_k^{(2)}}, \tag{12a}$$

$$r=\frac{(1-e^{2ikL})\Gamma_1\Gamma_2-ie^{2ikL}\Gamma_2\delta_k^{(1)}-i\Gamma_1\delta_k^{(2)}}{(-1+e^{2ikL})\Gamma_1\Gamma_2+i\left(\Gamma_1\delta_k^{(2)}+\Gamma_2\delta_k^{(1)}\right)+\delta_k^{(1)}\delta_k^{(2)}}. \tag{12b}$$

There is no splitting in the reflection spectrum. Figure 6 shows R and T as a function of Δ_k for asymmetric coupling. Both the cases $kL\neq 0$ and $kL=0$ are shown. It exhibits clearly that the DDI splits the reflection and transmission spectrum.

V. MULTIPLE QUANTUM EMITTERS

If one QE couples to the waveguide, only the photon with frequency equal to the transition frequency of the QE reflects perfectly. Based on the coupled-resonator waveguide, Chang *et al.* proposed using many atoms individually in the resonators to realize perfect reflection of a single photon in a wide band of frequency [62]. Here, we exhibit that the DDI can broaden the bandwidth. Figure 7 shows the single-photon reflection spectra where five QDs couple to the Ag nanowire. The separations between the two neighboring QDs are 32.75 nm [Figs. 7(a) and 7(b)], 52.95 nm [Figs. 7(c) and 7(d)], and 105.9 nm [Figs. 7(e) and 7(f)], where the distance-dependent Ω is considered, which can be found in Fig. 5(a). In Fig. 7(a), the width is broadened by about 2.5 times that without DDI. Furthermore, the maximum of the peak in the reflection spectra is also enhanced. Figure 6(c) shows that the bandwidth of the reflection spectrum is broadened and the peak is increased even though L reaches $\lambda_{sp}/4(kL=\pi/2)$. However, if L further increases to $\lambda_{sp}/2(kL=\pi)$, the numerical results with and without DDI are almost indistinguishable, as shown in Fig. 7(e).

To exhibit how DDI broadens reflection spectra clearly, we present R as a function of Δ_k and kL with and without DDI in Fig. 8. When $kL\approx 0.31\pi$, Ω is about $23.08\Gamma_0$. It can affect the scattering spectrum strongly, as we discussed above. It shows

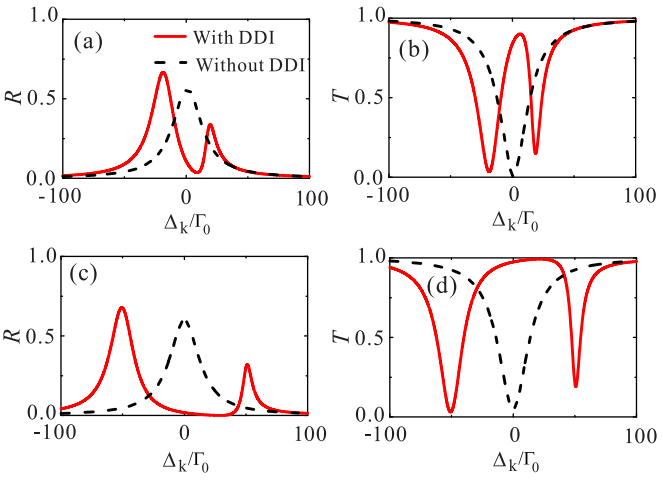

FIG. 6. The single-photon reflection and transmission spectra for the two QDs placed in different locations. In (a) and (b), and $\vec{r}_2(x,y,z)=(20\,\text{nm},\ 37\,\text{nm},\ 0)$, corresponding to $kL=0.19\pi$. $\Gamma_1=11.03\Gamma_0$ and $\Gamma_{01}^{'}=6.86\Gamma_0$, $\Gamma_2=1.06\Gamma_0$, $\Gamma_{02}^{'}=1.26\Gamma_0$, and $\Omega=-20.79\Gamma_0$. In (c) and (d), $\vec{r}_1(x,y,z)=(0,\ 17\,\text{nm},\ 0)$ and $\vec{r}_2(x,y,z)=(0,\ 49.75\,\text{nm},\ 0)$, corresponding to $kL=0$. $\Gamma_1=11.03\Gamma_0$ and $\Gamma_{01}^{'}=6.86\Gamma_0$, $\Gamma_2=0.33\Gamma_0$, $\Gamma_{02}^{'}=1.12\Gamma_0$, and $\Omega=-50.71\Gamma_0$.

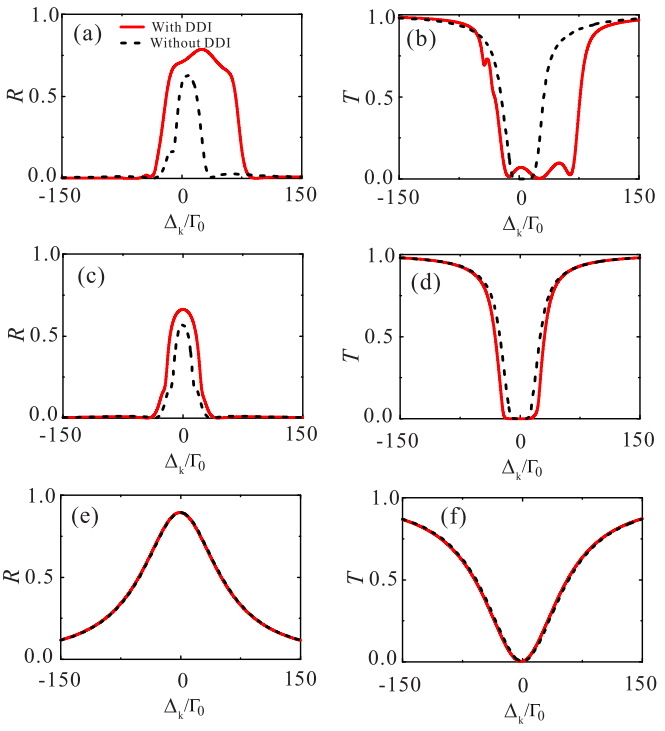

FIG. 7. The single-photon reflection and transmission spectra for the case of five QDs coupled to the nanowire. The separations between two neighboring QDs along the x direction are (a), (b) $\lambda_{qd}/20=32.75\,\text{nm}$, (c), (d) $\lambda_{sp}/4=52.95\,\text{nm}$, and (e), (f) $\lambda_{sp}/2=105.9\,\text{nm}$. In the calculations, $\Gamma=11.03\Gamma_0$ and $\Gamma_0^{'}=6.86\Gamma_0$. The DDI coupling for each pair has been calculated using Fig. 5(a). As an example, in (a), the coupling between the first and second is $23.08\Gamma_0$ and between the first and third is $2.60\Gamma_0$.

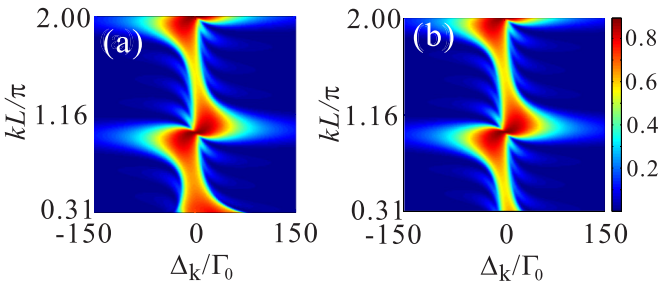

FIG. 8. The single-photon reflection spectra as a function of Δ_k and kL (a) with and (b) without DDI. In the calculations, $\Gamma = 11.03\Gamma_0$ and $\Gamma_0^{'} = 6.86\Gamma_0$. The DDI coupling was calculated using Fig. 5(a).

that the red region in the direction of Δ_k in Fig. 8(a) is much larger than in Fig. 8(b). However, when kL increases to more than π, the influence of DDI can be neglected; then there is no obvious difference between Figs. 8(a) and 8(b).

VI. CONCLUSIONS

In summary, we have investigated single-photon scattering properties in a one-dimensional waveguide coupled to an array of QEs with DDI by using a real-space Hamiltonian. For the case of the chain consisting of two QEs with symmetric coupling, the reflection spectrum splits into two peaks due to the DDI; however, the splitting depends on both the DDI coupling and the spatial separation between the two QEs along the photon propagation direction in waveguide. The spectra also display the Fano interference minimum. With two QEs, there are new pathways which lead to transmission and reflection. For example, a new pathway will consist of the radiation, after being scattered by QE1, interacting with QE2; the scattered radiation from QE2 interacts back with QE1. Thus, the transmitted wave has an additional contribution from this pathway. The new pathways result in a Fano minimum. For both symmetric and asymmetric couplings, the DDI can induce reflection spectrum splitting. The distance between the two peaks in the reflection spectrum depends on the DDI strength strongly in both symmetric and asymmetrical coupling cases. DDI can also broaden the frequency bandwidth of the high reflection probability of a single photon when many QEs couple to the waveguide. Our results may find applications in design of single-photon devices and quantum-information processing.

ACKNOWLEDGMENTS

M.T.C. acknowledges discussions with Dr. Zeyang Liao, and support from the Anhui Provincial Natural Science Foundation under Grants No. 1608085MA09 and No. 1408085QA22, and the China Scholarship Council. G.S.A. thanks the Biophotonics initiative of the Texas A&M University for support.

[1] H. Walther, B. T. H. Varcoe, Berthold-Georg Englert, and T. Becker, Cavity quantum electrodynamics, Rep. Prog. Phys. **69**, 1325 (2006).
[2] A. Reiserer and G. Rempe, Cavity-based quantum networks with single atoms and optical photons, Rev. Mod. Phys. **87**, 1379 (2015).
[3] D. E. Chang, A. S. Sørensen, P. R. Hemmer, and M. D. Lukin, Quantum Optics with Surface Plasmons, Phys. Rev. Lett. **97**, 053002 (2006).
[4] C.-L. Hung, S. M. Meenehan, D. E. Chang, O. Painter, and H. J. Kimble, Trapped atoms in one-dimensional photonic crystals, New J. Phys. **15**, 083026 (2013).
[5] A. V. Akimov, A. Mukherjee, C. L. Yu, D. E. Chang, A. S. Zibrov, P. R. Hemmer, H. Park, and M. D. Lukin, Generation of single optical plasmons in metallic nanowires coupled to quantum dots, Nature (London) **450**, 402 (2007).
[6] H. Wei, D. Ratchford, X. Li, H. Xu, and C.-K. Shih, Propagating surface plasmon induced photon emission from quantum dots, Nano Lett. **9**, 4168 (2009).
[7] A. Huck, S. Kumar, A. Shakoor, and U. L. Andersen, Controlled Coupling of a Single Nitrogen-Vacancy Center to a Silver Nanowire, Phys. Rev. Lett. **106**, 096801 (2011).
[8] T. M. Babinec, B. J. M. Hausmann, M. Khan, Y. Zhang, J. R. Maze, P. R. Hemmer, and M. Lončar, A diamond nanowire single-photon source, Nat. Nanotechnol. **5**, 195 (2010).
[9] J. Claudon, J. Bleuse, N. S. Malik, M. Bazin, P. Jaffrennou, N. Gregersen, C. Sauvan, P. Lalanne, and J.-M. Gérard, A highly efficient single-photon source based on a quantum dot in a photonic nanowire, Nat. Photon. **4**, 174 (2010).
[10] O. Astafiev, A. M. Zagoskin, A. A. Abdumalikov, Jr., Yu. A. Pashkin, T. Yamamoto, K. Inomata, Y. Nakamura, and J. S. Tsai, Resonance fluorescence of a single artificial atom, Science **327**, 840 (2010).
[11] I.-C. Hoi, C. M. Wilson, G. Johansson, T. Palomaki, B. Peropadre, and P. Delsing, Demonstration of a Single-Photon Router in the Microwave Regime, Phys. Rev. Lett. **107**, 073601 (2011).
[12] R. Yalla, M. Sadgrove, K. P. Nayak, and K. Hakuta, Cavity Quantum Electrodynamics on a Nanofiber Using a Composite Photonic Crystal Cavity, Phys. Rev. Lett. **113**, 143601 (2014).
[13] A. Javadi, I. Söllner, M. Arcari, S. Lindskov Hansen, L. Midolo, S. Mahmoodian, G. Kiršanskė, T. Pregnolato, E. H. Lee, J. D. Song, S. Stobbe, and P. Lodahl, Single-photon non-linear optics with a quantum dot in a waveguide, Nat. Commun. **6**, 8655 (2015).
[14] A. Goban, C.-L. Hung, J. D. Hood, S.-P. Yu, J. A. Muniz, O. Painter, and H. J. Kimble, Superradiance for Atoms Trapped along a Photonic Crystal Waveguide, Phys. Rev. Lett. **115**, 063601 (2015).
[15] A. Sipahigil, R. E. Evans, D. D. Sukachev, M. J. Burek, J. Borreǵaard, M. K. Bhaskar, C. T. Nǵuyen, J. L. Pacheco, H. A. Atikian, C. Meuwly, R. M. Camacho, F. Jelezko, E. Bielejec, H. Park, M. Lončar, and M. D. Lukin, An integrated diamond nanophotonics platform for quantum-optical networks, Science **354**, 847 (2016).
[16] J. T. Shen and S. Fan, Coherent photon transport from spontaneous emission in one-dimensional waveguide, Opt. Lett. **30**, 2001 (2005).
[17] L. Zhou, Z. R. Gong, Y.-X. Liu, C. P. Sun, and F. Nori, Controllable Scattering of a Single Photon inside a One-Dimensional Resonator Waveguide, Phys. Rev. Lett. **101**, 100501 (2008).

[18] J.-Q. Liao, J.-F. Huang, Y.-X. Liu, L.-M. Kuang, and C. P. Sun, Quantum switch for single-photon transport in a coupled superconducting transmission-line-resonator array, Phys. Rev. A **80**, 014301 (2009).

[19] D. Witthaut and A. S. Sørensen, Photon scattering by a three-level emitter in a one-dimensional waveguide, New J. Phys. **12**, 043052 (2010).

[20] N. C. Kim, J.-B. Li, Z.-J. Yang, Z.-H. Hao, and Q.-Q. Wang, Switching of a single propagating plasmon by two quantum dots system, Appl. Phys. Lett. **97**, 061110 (2010).

[21] N.-C. Kim, M.-C. Ko, and Q.-Q. Wang, Single plasmon switching with n quantum dots system coupled to one-dimensional waveguide, Plasmonics **10**, 611 (2015).

[22] M.-T. Cheng, X.-S. Ma, M.-T. Ding, Y.-Q. Luo, and G.-X. Zhao, Single-photon transport in one-dimensional coupled-resonator waveguide with local and nonlocal coupling to a nanocavity containing a two-level system, Phys. Rev. A **85**, 053840 (2012).

[23] Z. Liao, X. Zeng, S.-Y. Zhu, and M. S. Zubairy, Single-photon transport through an atomic chain coupled to a one-dimensional nanophotonic waveguide, Phys. Rev. A **92**, 023806 (2015).

[24] W.-B. Yan and H. Fan, Control of single-photon transport in a one-dimensional waveguide by a single photon, Phys. Rev. A **90**, 053807 (2014).

[25] C.-H. Yan and L. F. Wei, Photonic switches with ideal switching contrasts for waveguide photons, Phys. Rev. A **94**, 053816 (2016).

[26] T. S. Tsoi and C. K. Law, Quantum interference effects of a single photon interacting with an atomic chain inside a one-dimensional waveguide, Phys. Rev. A **78**, 063832 (2008).

[27] T. S. Tsoi and C. K. Law, Single photon scattering on Λ type three-level atoms in a one-dimensional waveguide, Phys. Rev. A **80**, 033823 (2009).

[28] J. T. Shen and S. Fan, Theory of single-photon transport in a single-mode waveguide. I. Coupling to a cavity containing a two-level atom, Phys. Rev. A **79**, 023837 (2009).

[29] J. T. Shen and S. Fan, Theory of single-photon transport in a single-mode waveguide. II. Coupling to a whispering gallery resonator containing a two-level atom, Phys. Rev. A **79**, 023838 (2009).

[30] D. Roy, Two-Photon Scattering by a Driven Three-Level Emitter in a One-Dimensional Waveguide and Electromagnetically Induced Transparency, Phys. Rev. Lett. **106**, 053601 (2011).

[31] P. Longo, P. Schmitteckert, and K. Busch, Few-Photon Transport in Low-Dimensional Systems: Interaction-Induced Radiation Trapping, Phys. Rev. Lett. **104**, 023602 (2010).

[32] H. Zheng, D. J. Gauthier, and H. U. Baranger, Cavity-Free Photon Blockade Induced by Many-Body Bound States, Phys. Rev. Lett. **107**, 223601 (2011).

[33] Y.-L. L. Fang, and H. U. Baranger, Waveguide QED: Power spectra and correlations of two photons scattered off multiple distant qubits and a mirror, Phys. Rev. A **91**, 053845 (2015).

[34] M. Bradford, K. C. Obi, and J.-T. Shen, Efficient Single-Photon Frequency Conversion Using a Sagnac Interferometer, Phys. Rev. Lett. **108**, 103902 (2012).

[35] L. Neumeier, M. Leib, and M. J. Hartmann, Single-Photon Transistor in Circuit Quantum Electrodynamics, Phys. Rev. Lett. **111**, 063601 (2013).

[36] L. Zhou, L.-P. Yang, Y. Li, and C. P. Sun, Quantum Routing of Single Photons with a Cyclic Three-Level System, Phys. Rev. Lett. **111**, 103604 (2013).

[37] X. Li and L. F. Wei, Designable single-photon quantum routings with atomic mirrors, Phys. Rev. A **92**, 063836 (2015).

[38] M.-T. Cheng, X.-S. Ma, J.-Y. Zhang, and B. Wang, Single photon transport in two waveguides chirally coupled by a quantum emitter, Opt. Express **24**, 19988 (2016).

[39] E. Sanchez-Burillo, D. Zueco, J. J. Garcia-Ripoll, and L. Martin-Moreno, Scattering in the Ultrastrong Regime: Nonlinear Optics with One Photon, Phys. Rev. Lett. **113**, 263604 (2014).

[40] S. Derouault and M. A. Bouchene, One-photon wave packet interacting with two separated atoms in a one-dimensional waveguide: Influence of virtual photons, Phys. Rev. A **90**, 023828 (2014).

[41] Y. S. Greenberg and A. A. Shtygashev, Non-Hermitian Hamiltonian approach to the microwave transmission through a one-dimensional qubit chain, Phys. Rev. A **92**, 063835 (2015).

[42] D. Roy, C. M. Wilson, and O. Firstenberg, Strongly interacting photons in one-dimensional continuum, arXiv:1603.06590.

[43] K. Xia, G. Lu, G. Lin, Y. Cheng, Y. Niu, S. Gong, and J. Twamley, Reversible nonmagnetic single-photon isolation using unbalanced quantum coupling, Phys. Rev. A **90**, 043802 (2014).

[44] D. E. Chang, A. S. Sørensen, E. A. Demler, and M. D. Lukin, A single-photon transistor using nanoscale surface plasmons, Nat. Phys. **3**, 807 (2007).

[45] O. Kyriienko and A. S. Sørensen, Continuous-Wave Single-Photon Transistor Based on a Superconducting Circuit, Phys. Rev. Lett. **117**, 140503 (2016).

[46] Z. Liao, H. Nha, and M. S. Zubairy, Single-photon frequency-comb generation in a one-dimensional waveguide coupled to two atomic arrays, Phys. Rev. A **93**, 033851 (2016).

[47] A. Albrecht, T. Caneva, and D. E. Chang, Changing optical band structure with single photons, arXiv:1610.00988.

[48] N. V. Corzo, B. Gouraud, A. Chandra, A. Goban, A. S. Sheremet, D. V. Kupriyanov, and J. Laurat, Large Bragg Reflection from One-Dimensional Chains of Trapped Atoms near a Nanoscale Waveguide, Phys. Rev. Lett. **117**, 133603 (2016).

[49] H. L. Sørensen, J.-B. Béguin, K. W. Kluge, I. Iakoupov, A. S. Sørensen, J. H. Müller, E. S. Polzik, and J. Appel, Coherent Backscattering of Light Off One-Dimensional Atomic Strings, Phys. Rev. Lett. **117**, 133604 (2016).

[50] C. Sayrin, C. Junge, R. Mitsch, B. Albrecht, D. O'Shea, P. Schneeweiss, J. Volz, and A. Rauschenbeutel, Nanophotonic Optical Isolator Controlled by the Internal State of Cold Atoms, Phys. Rev. X **5**, 041036 (2015).

[51] G. S. Agarwal, *Quantum Optics* (Cambridge University Press, New York, 2013).

[52] W. Tian, B. Chen, and G. Tong, Controlling single-photon transport in a one-dimensional resonator waveguide by interatomic dipole-dipole interaction, Int. J. Mod. Phys. B **26**, 1250194 (2012).

[53] M.-T. Cheng, X.-S. Ma, and X. Wang, Transmission characteristics of waveguide-coupled nanocavity embedded in two atoms with dipole-dipole interaction, Chin. Phys. Lett. **31**, 014202 (2014).

[54] X.-Y. Yu and J.-H. Li, The effect of dipole-dipole interactions on the single-photon transmission spectrum, Eur. Phys. J. D **67**, 177 (2013).

[55] H. Zheng and H. U. Baranger, Persistent Quantum Beats and Long-Distance Entanglement from Waveguide-Mediated Interactions, Phys. Rev. Lett. **110**, 113601 (2013).

[56] G.-Y. Chen, N. Lambert, C.-H. Chou, Y.-N. Chen, and F. Nori, Surface plasmons in a metal nanowire coupled to colloidal quantum dots: Scattering properties and quantum entanglement, Phys. Rev. B **84**, 045310 (2011).

[57] C. Gonzalez-Ballestero, E. Moreno, and F. J. Garcia-Vidal, Generation, manipulation, and detection of two-qubit entanglement in waveguide QED, Phys. Rev. A **89**, 042328 (2014).

[58] P. Facchi, M. S. Kim, S. Pascazio, F. V. Pepe, D. Pomarico, and T. Tufarelli, Bound states and entanglement generation in waveguide quantum electrodynamics, Phys. Rev. A **94**, 043839 (2016).

[59] I. M. Mirza and J. C. Schotland, Multiqubit entanglement in bidirectional-chiral-waveguide QED, Phys. Rev. A **94**, 012302 (2016).

[60] Z. Liao, H. Nha, and M. S. Zubairy, Dynamical theory of single photon transport in a one-dimensional waveguide coupled to identical and non-identical emitters, Phys. Rev. A **94**, 053842 (2016); see also X. Li and L. F. Wei, Probing a single dipolar interaction between a pair of two-level quantum system by scatterings of single photons in an aside waveguide, Opt. Commun. **366**, 163 (2016).

[61] M.-T. Cheng and Y.-Y. Song, Fano resonance analysis in a pair of semiconductor quantum dots coupling to a metal nanowire, Opt. Lett. **37**, 978 (2012).

[62] Y. Chang, Z. R. Gong, and C. P. Sun, Multiatomic mirror for perfect reflection of single photons in a wide band of frequency, Phys. Rev. A **83**, 013825 (2011).